MANSOURA JOURNAL OF CHEMISTRY
Official Journal of Faculty of Science, Mansoura University, Egypt
E-mail: scimag@mans.edu.eg ISSN: 2974-4938

Preparation and characterization of modified mesoporous MCM-41for removal of organic and inorganic pollutants.

Atef. M. M. Farag[a], Shady M. Eldefrawy[b], Dlal E. Dewan[a], A. I. Ahmed[b].*

[a] *Central Lab.of drinking water, Dakahliya water company.*

[b] *Chemistry Department, Faculty of science, Mansoura university.*

* Correspondence to: atef_shita1981@yahoo.com, *01002672819*)

Received:27/4/2025
Accepted:10/5/2025

Abstract: Here, sulfamic acid (SA) was added to mesoporous silica (MCM-41) to successfully remove the metal ions (Cu and Mn) and methylene blue (MB) dye. SA/MCM-41 composites with different weight compositions of SA were successfully made using the straightforward impregnation method. Several techniques, including SEM, EDX, XRD, BET, and FT-IR spectroscopy, were used to characterize the as-synthesized composites. Non-aqueous potentiometric titration has been used to investigate the acidic characteristics of the composites. MCM-41's ordered mesoporous structure with amorphous lattice is confirmed by XRD studies, and even after treatment with SA, its mesoporous structure remained unchanged. The high surface area of 10SA-MCM-41 (211.7 m2/g) decreased when sulfamic acid was added, reaching 5.38 m2/g at 50%. SA-MCM-41. The prepared composites' acidic strength was gradually enhanced by increasing the SA content to 35 weight percent SA/MCM-41. According to the tests, the as-synthesized composites could remove 50–55% of the MB dye, 70–75% of the Cu ions, and 60–65% of the Mn ions.

keywords: sulfamic acid**,** mesoporous silica**,** removal of heavy metal**,** methylene blue dye

1.Introduction

Researchers have been focusing more on green and ecologically friendly organic processes recently[1, 2]. In this regard, solid heterogeneous catalysts have garnered a lot of attention from both economic and environmental perspectives because they offer more benefits than homogeneous catalysts, including shorter reaction times, multiple reuses, decreased equipment corrosion, and reduced waste production [3-5]. Thus, extensive attempts are underway to replace traditional liquid acid catalysts with heterogeneous solid acid catalysts [6]. Because of their important features, mesoporous materials have recently been employed as heavy metal and dye adsorbents [7], catalyst supports [8-12], and heterogeneous solid acid catalysts. Practically speaking, Mobil scientists created organized mesoporous materials for the first time in 1992. [13, 14]. Because of their high surface area, consistently sized nanochannels, controllable pore size (2–10 nm), and great thermal stability [8, 15-19]. MCM-41 materials were a viable support. Adsorption, electrical and optical devices, medication delivery, separation, photocatalysis, chemical sensors, and nanotechnology are just a few of its many potential uses. [12, 20-24].One of the main drawbacks of mesoporous MCM-41 is that it only shows weak hydrogen-bonded sites and no Brønsted acid sites [25-27]. Consequently, it is imperative to enhance the acid strength by changing the surface or adding potent acid moieties like citric acid and heteropoly acids[28, 29], sulfated zirconia[30, 31], or sulfate ions[32, 33] inside the MCM-41 inner channels. The surface acidity and catalytic performance are enhanced by the Brønsted acid sites created by this alteration. NH_2SO_3H, SA, or sulfamic acid is regarded as an inexpensive, economically accessible, and efficient acid because of its many qualities, including being a nonvolatile solid, odorless, and non-hygroscopic substance. Thus, in a variety of processes, including esterification[34], ketal production or

acetalization[35], transesterification of ketoester[36], tetrahydropyranylation of In the alcohol synthesis [37] and nitrile synthesis [38], SA functions as an efficient heterogeneous solid acid catalyst. Because this class of heterocyclic compounds is widely used in a variety of possible applications, including laser technologies [39], dye synthesis [40], and pH-sensitive fluorescent materials [41], xanthene derivatives are among the most physiologically and pharmaceutically active substances. The use of commercial activated carbon adsorption technology has gained recognition and has established itself as one of the most successful methods for removing dye effluents. However, the manufacture and renewal of activated carbon are often expensive. Therefore, alternate materials include waste materials, agricultural by-products, and some natural adsorbents (such as clays and clay minerals, cellulosic materials, chitin, and chitosan). Because of their distinct mesoporous pore structure, which is characterized by high surface area and pore volume, mesoporous molecular sieves, such as surfactant-modified FSM-16 [19], MCM-22, and silane-modified MCM-41 [42], have been recognized as suitable adsorbents for the removal of dyes from wastewater. Heavy metal ion removal from wastewater has been the focus of much industrial research. These contaminants, which are present in the effluents from the production of chemicals, paints, and coatings, pose a serious risk to both human health and the environment. There are numerous methods for eliminating heavy metals from water. Due to its affordability and ease of use, Adsorption has become popular. Heavy metals are removed using various adsorption materials, including activated carbon and inexpensive adsorbents such as peat and agricultural waste. These materials' poor loading capacities and very weak interactions with metallic cations are just two of their many disadvantages. Many researchers have created surface-modified mesoporous materials and organoclays as functionalized adsorbents to overcome this drawback [43].

Here, mesoporous MCM-41 was successfully prepared using the standard procedure and modified by adding different amounts of sulfamic acid (10, 15, 25, 35, and 50 weight percent) via impregnation techniques. Several techniques, including XRD, EDX, SEM, FT-IR, and BET measurements, were used to characterize the asynthesized composites. Adsorption was used to test the as-synthesized catalysts' adsorptive capabilities of inorganic pollutants such as Cu and Mn ions and organic pollutants like methylene blue dye.

2. Experimental

2.1. Materials

Methylene blue, sulfuric acid, sulfamic acid, analytical grade cetyltrimethyl ammonium bromide (CTAB), Na2SiO3.5H2O, and Cu and Mn ion standers were all acquired from Merck and Aldrich.

2.2. Preparation of MCM-41

With a minor modification [14], mesoporous MCM-41 was obtained using the procedure described in the literature with 70 g of Na_2SiO_3. Following the dissolution of $5H_2O$ in 200 ml of H_2O and stirring at 35°C, 2M H_2SO_4 was used to produce an aqueous solution, and the liquid was agitated for 30 min to reduce the pH down to 11. Then, 18 g of CTAB was added dropwise to the gel after dissolving it in 60 mL of water, followed by stirring for half an hour. The finished product was filtered, cleaned several times, dried at 120°C for 12 h, and then calcined at 550°C for 4 h at a rate of 5°C/min.

2.3. Preparation of Sulfamic acid@MCM-41

The produced MCM-41 (1 g) was mixed with several weight percentages of sulfamic acid (10, 15, 25, 35, and 50 wt%) at 80 ◦C for 6 h and then impregnated for 48 h [44-47] in accordance with our earlier literature, with minor modifications[48]. After washing, the filtrate was dried at 100 °C. The prepared samples were referred to as 10SA-MCM, 15SA-MCM, 25SA-MCM, 35SA-MCM, and 50SA-MCM based on the percentage of sulfamic acid.

2.4. Catalyst characterization

Employing Cu Kα radiation (λ = 1.540 Å), X-ray diffraction patterns (XRD) of unaltered and modified MCM-41 with different sulfamic acid weight contents were obtained utilizing a Philips X'Pert diffractometer. The FT-IR analysis of the synthesized composites as performed utilizing a Shimadzu FT-IR spectrophotometer with a

resolution of 4 cm-1 and 128 scans across wavelengths ranging from 400 to 4000cm^{-1}. The surface structure of the synthesized catalysts as analyzed through scanning electron microscopy (SEM – JEOL JSM-6510LV) examination. The N2 adsorption-desorption isotherm was performed using a BELSORP-mini II device at -196◦C. Non-aqueous potentiometric titration was employed to explore the acidic properties of SA-MCM-41

2.5.Adsorption studies.

2.5.1 Removal of methylene blue dye from aqueous solutions

It was conducted by the addition of 0.01 g of the catalyst into a 50 ml of MB solution in a 100-ml stirred flask at temperature of 30 oC, the concentration of MB was calculated from its absorbance at 666 nm using calibration curve obtained by a UV-Vis spectrophotometer (Cintra 101). The % of removal calculated from the equation: -

$$\% \text{ Removal} = \frac{Co - Ct}{Co} \times 100$$

Were

Co the initial concentration of MB.

Ct the final concentration of MB.

2.5.2Removal of Cu and Mn ions from aqueous solutions

It was conducted by the addition of 0.01 g of the catalyst into a 50 ml of metal ion solution in a 100-ml stirred flask at temperature of 30 oC, the concentration of metal ion was calculated from its absorbance at atomic absorption using calibration curve obtained by a flame atomic absorption (AA 240FS). The % of removal calculated from the equation: -

$$\% \text{ Removal} = \frac{Co - Ct}{Co} \times 100$$

Were

Co the initial concentration of metal ion.

Ct the final concentration of metal ion.

Results and discussion

3.1. X-ray diffraction pattern (XRD)

The X-ray diffraction technique was used in this work to determine MCM-41's crystallinity and to monitor any potential changes in the structural phase % and crystallite size that might arise from fluctuations in the sulfamic acid amounts. The following samples were chosen for this investigation: 15SA-MCM, 25SA-MCM, 35SA-MCM, and 50SA-MCM. As seen in Fig. 1, the low crystallinity for sulfamic acid impregnated samples certifies that the MCM-41 framework remained amorphous even as the sulfamic acid level increased.

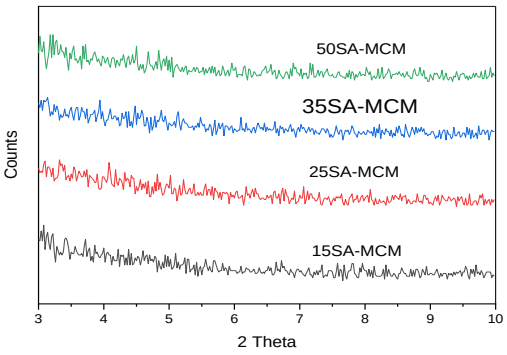

Fig.1 Low angle X-ray diffraction patterns of MCM-41 with different concentration of sulfamic acid calcined at 400 ^{o}C.

3.2. SEM and SEM-EDX analysis

Using a SEM fitted with an EDX detector, the morphology and elemental makeup of MCM-41 and 50SA-MCM were investigated and are displayed in Fig. 2. The produced materials' SEM pictures showed comparable particle morphology. To map the presence of sulfuric acid, EDX was used. 50SA-MCM was not a physical combination, according to the EDX picture, but sulfamic acid was evenly distributed across the MCM-41 surface. Sulfamic acid alteration caused the diffraction peaks associated with the S, N, and O elements to be seen[49].

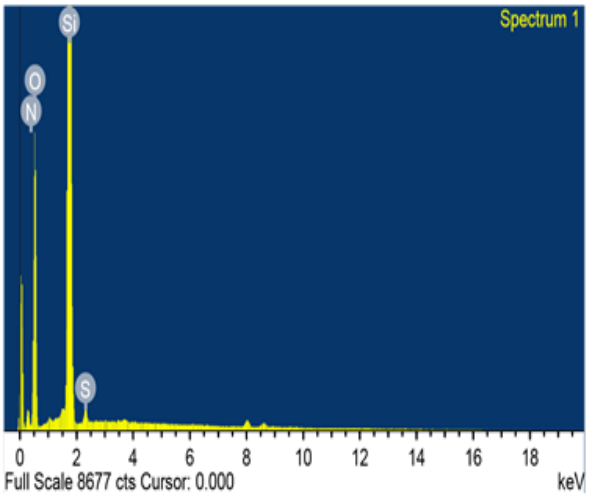

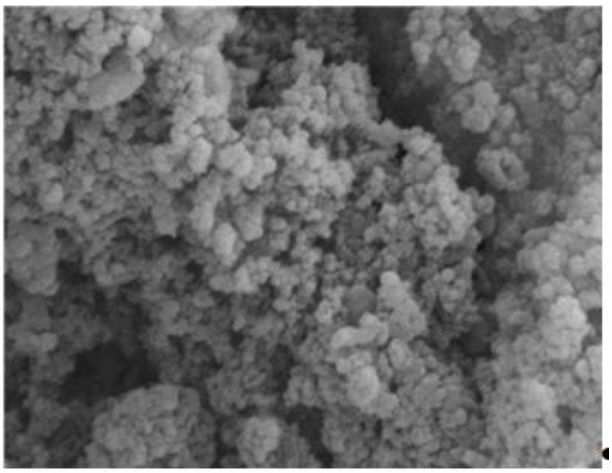

Fig 2. SEM and EDX for 10SA-MCM

3.3. FT-IR spectroscopy

Figure 3 showed the FT-IR of the as-synthesised composites. The O–H stretching and bending vibrations of water molecules are shown by the big peaks at 3462 and 1638 cm-1, respectively [50, 51]. The symmetric and asymmetric stretching of the Si–O–Si groups was associated with the broad bands at 1060 and 809 cm-1. Defective Si–OH groups are associated with the band at 966 cm-1, while the bending vibration of the Si–O group is associated with the absorption peak at 468 cm-1[52]. No discernible change was observed following the sulfamic acid adjustment; this could be because the sulfamic acid was dispersed uniformly throughout the catalyst.

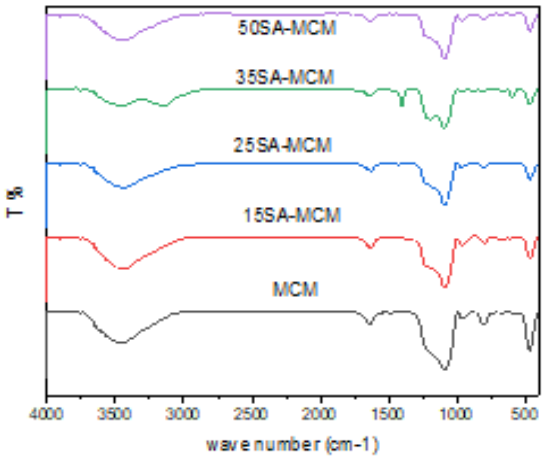

Fig 3. FT-IR for prepared samples

3.4. BET Measurement

The N_2 adsorption-desorption isotherms of the as-synthesised composites were displayed in Figure 4. A typical type IV adsorption isotherm with a hysteresis loop H2 is displayed by all of the manufactured catalysts, according to IUPAC, indicating that the produced composite has retained its uniform mesoporous structure [53]. The mesopore walls of the generated samples were coated with a monolayer of nitrogen under low pressure. But when the relative pressure increases, as is common with capillary condensation, the isotherms rise (at about P/Po ca. 0.4). Mesopores. Lastly, multilayer adsorption on the exterior surface is the cause of the plateau zone at higher relative pressures. Additionally, the adsorbed volume curve rose with the initial weight percentage of 10% and decreased with the greater sulfamic acid percentage. Acid added to MCM-41, indicating that the pore volume may be impacted by the addition of sulfamic acid to MCM-41 frameworks. MCM-41 has a surface area of 142.7 m^2/g, which rises to 211.7 m^2/g and then decreases with additional sulfamic acid addition until it reaches 5.38 m^2/g at 50SA-MCM. This could be because sulfamic acid is deposited on the outside of MCM-41 and inside its pores [49].

Table (1) Surface area of the investgated samples.

Catalyst	$S_{BET} m^2/g$	$S_a m^2/g$
MCM	142.7	172.7
10SA-MCM	211.7	220.4
25SA-MCM	12.81	12.34
50SA-MCM	5.38	4.02

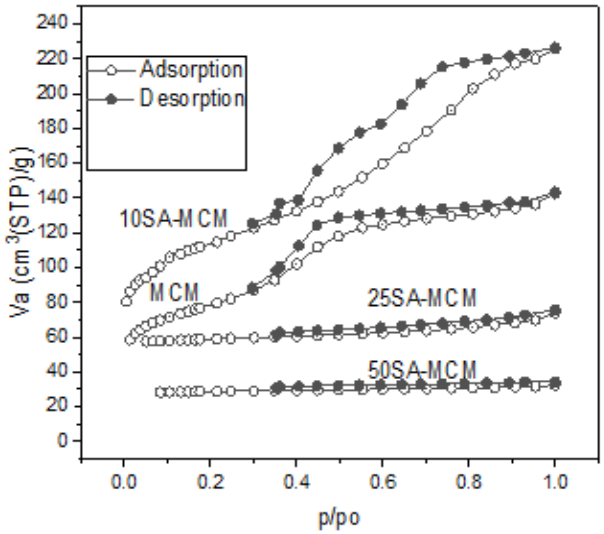

Fig.4. Adsorption-desorption isotherms of nitrogen at -196 ^oC on prepared samples.

3.5.Acidity measurements

3.5.1. Non-aqueous potentiometric titration

Using non-aqueous titration, the produced sample's acidic qualities were investigated [54].

As shown in Fig. 5, this procedure was carried out by measuring the electrode potential (mV) in relation to the volume of n-butylamine added over the catalysts as (mmol n-butylamine/g catalyst). The following relation was used to get the total number of acid sites per gram: (mequiv./g) ×N × 1000 (where N is Avogadro's number) = total number of acid sites/g [46, 55]. The as-synthesised composites' overall acidity rose as the sulfamic acid concentration rose, reaching its highest value at 35SA-MCM (Ei = +312 mV), as shown in Fig. 5 and Table 2. The findings showed that the MCM-41 surface had a good distribution of sulfate groups. However, the surface acidity dropped once more. following 35SA-MCM, which could be the result of SA crystals building up on MCM-41's surface [48].

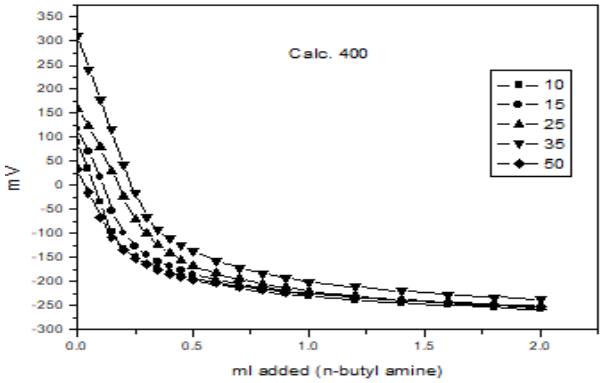

Fig.5 sulfamic acid concentration on total no of acid sites at 400 ^{o}C

Table (2) Acidic properties of the investgated samples.

Sample Name	E_o (mV)	No.of mmol n-butylamine/g	No. of acid sites/g 10^{19}
10SA/MCM-41 **(II)**	89.50	0.124	7.46
15SA/MCM-41 **(II)**	118.25	0.139	8.37
25SA/MCM-41 **(II)**	158.41	0.183	11.02
35SA/MCM-41 **(II)**	312.60	0.202	12.16
50SA/MCM-41 **(II)**	34.60	0.126	7.59

3.7. Removal of methelene blue from aqueous media .

The interaction between the basic dye and the hydroxyl group on the surface of MCM-41, which is made up of OH group ,and oxygen bridge that function as adsorption site, is what gives MCM-41 its ability to adsorb methelene blue (MB). Understanding the properties of these many adsorption sites is crucial for adsorption operations. OH groups can be classified as (i) isolated free silanol (-SiOH), (ii) germinal free silanol (-$Si(OH)_2$), and (iii) vicinal or bridging or OH groups bound through the hydrogen bond. In general, OH groups function as foci for adsorption by creating hydrogen bonds with the adsorbate. Furthermore, siloxane groups or -Si-O-Si- bridges with oxygen atoms on the surface make up MCM-41. Overall, it was shown that the relationship between the MCM-41 and the integrated dye molecule were extremely potent, as were the polar atoms N and S, as shown in scheme (1) [56, 57].

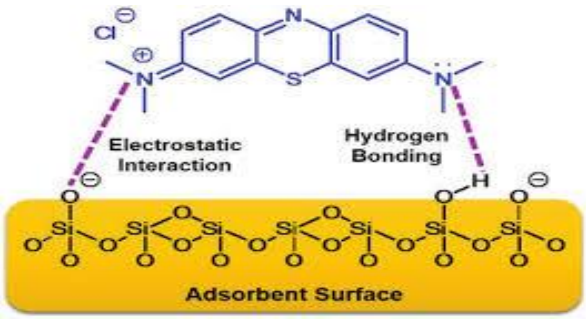

Scheme 1 :Represent the interaction between methelene blue and MCM-41.

When MCM-41 is created without sulfamic acid modification, it does not exhibit adsorption characteristics; but, when changed, it does. The impact of contact time on methylene blue (MB) adsorption onto modified MCM-41 was investigated at an initial MB concentration of 100 mg/L at 30 oC. It seems that adsorption progressively rises as contact time increases until it reaches the equilibrium duration, which is about equivalent to 8 hours.

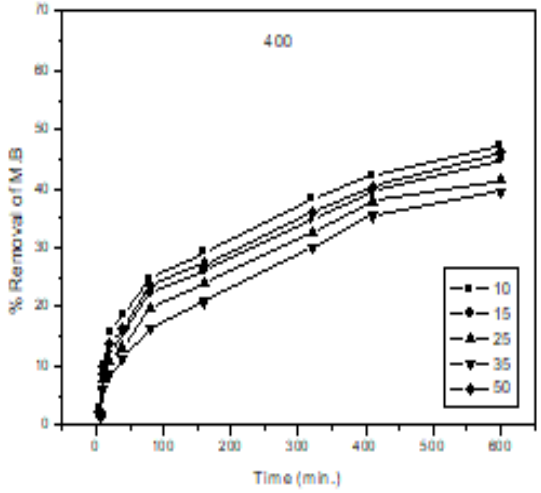

Fig 6 effect of time on removal of MB removal

3.8. Removal of Cu^{2+} and Mn^{2+} ions from aqueous media.

When MCM-41 is created without sulfamic acid modification, it does not exhibit adsorption characteristics; but, when changed, it does. Up to pH = 9, the number of Cu2+ and Mn2+ ions that are eliminated increases steadily. After pH = 9, the amount of Cu and Mn ions that precipitate decreases. The removal rises as the adsorbent weight increases to 0.8 mg/L, then falls, and then rises when the concentration of Mn and Cu ions increases to 30 mg/L, at which point it stabilizes. As the percentage of sulfamic acid increases, the elimination of ions decreases. The effect of contact time on ion adsorption onto modified MCM-41 was investigated at 30 oC with an initial ion concentration of 5 mg/L. It appears that adsorption progressively increases as in contact period till the equilibrium period, which is roughly one hour as shown in figure 7.

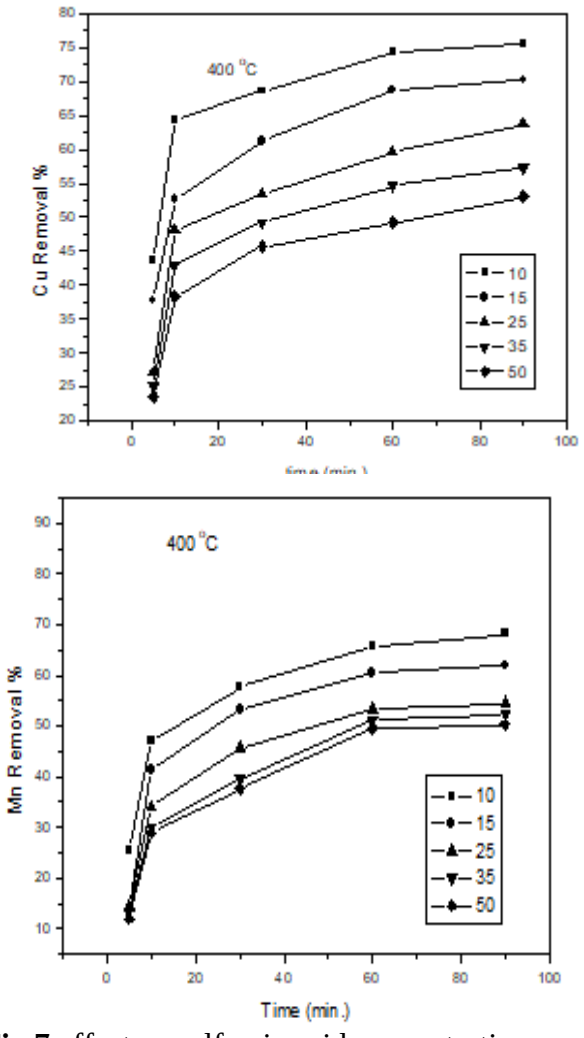

Fig 7 effect os sulfamic acid concentration on Mn and Cu removal

References

1. Hassan, S.M., A.I. Ahmed, and M.A. Mannaa, (2018) Structural, photocatalytic, biological and catalytic properties of SnO2/TiO2 nanoparticles. Ceramics International,. **44**(6): p. 6201-6211.
2. Mannaa, M.A., S. Hassan, and A.I. Ahmed, (2018) Synthesis and bioactivities of H3PW12O40/SnO2-TiO2 nanocomposite. *Int. J. Modern Chem,*. **10**(1): p. 69-79.
3. Kimura, M., T. Nakato, and T. Okuhara, (1997) .Water-tolerant solid acid catalysis of Cs2. 5H0. 5PW12O40 for hydrolysis of esters in the presence of excess water. Applied Catalysis A: General, **165**(1-2): p. 227-240.
4. Okuyama, K., et al., (2000) Water-tolerant catalysis of a silica composite of a sulfonic acid resin, Aciplex. Applied Catalysis A: General,. **190**(1-2): p. 253-260.
5. Okuhara, T., (2002) Water-tolerant solid acid catalysts. Chemical reviews,. **102**(10): p. 3641-3666.
6. El-Hakam, S., et al., (2013) *S*urface acidity and catalytic activity of sulfated titania supported on mesoporous MCM-41. *Int. J. Mod. Chem,*. **5**: p. 55-70.
7. Mannaa, M.A., H.M. Altass, and R.S. Salama, (2021) MCM-41 grafted with citric acid: The role of carboxylic groups in enhancing the synthesis of xanthenes and removal of heavy metal ions. Environmental Nanotechnology, Monitoring & Management,. **15**: p. 100410.
8. Nandhini, K.U., et al., (2006) Al-MCM-41 supported phosphotungstic acid: application to symmetrical and unsymmetrical ring opening of succinic anhydride. *Journal of Molecular Catalysis A: Chemical,*. **243**(2): p. 183-193.
9. Pham, S.T., et al., (2020) Role of Brønsted and Lewis acidic sites in sulfonated Zr-MCM-41 for the catalytic reaction of cellulose into 5-hydroxymethyl furfural. Reaction Kinetics, Mechanisms and Catalysis,. **130**: p. 825-836.
10. Ambursa, M.M., et al., (2017) Bimetallic Cu-Ni catalysts supported on MCM-41 and Ti-MCM-41 porous materials for

hydrodeoxygenation of lignin model compound into transportation fuels. Fuel Processing Technology,. **162**: p. 87-97.
11. Carriazo, D., et al., (2008) PMo or PW heteropoly acids supported on MCM-41 silica nanoparticles: Characterisation and FT-IR study of the adsorption of 2-butanol. *Journal of Solid State Chemistry*,. **181**(8): p. 2046-2057.
12. Naik, B., et al., (2017) Enhanced photocatalytic activity of nanoporous BiVO4/MCM-41 co-joined nanocomposites for solar energy conversion and environmental pollution abatement. *Journal of environmental chemical engineering*,. **5**(5): p. 4524-4530.
13. Beck, J.S., et al., (1992) A new family of mesoporous molecular sieves prepared with liquid crystal templates. *Journal of the American Chemical Society*,. **114**(27): p. 10834-10843.
14. Kresge, a.C., et al., (1992) Ordered mesoporous molecular sieves synthesized by a liquid-crystal template mechanism. nature,. **359**(6397): p. 710-712.
15. Ediati, R., et al., (2021) Synthesis of HKUST-1 with addition of Al-MCM-41 as adsorbent for removal of methylene blue from aqueous solution. Materials Today: Proceedings,. **46**: p. 1799-1806.
16. Rios, A.G., et al., (2020).Adsorption of anionic and cationic dyes into shaped MCM-41. Adsorption, **26**: p. 75-88.
17. He, D., et al., (2013) Synthesis of titanium containing MCM-41 and its application for catalytic hydrolysis of cellulose. Powder technology,. **249**: p. 151-156.
18. Bayramoglu, G. and M.Y. Arica, (2016) MCM-41 silica particles grafted with polyacrylonitrile: Modification in to amidoxime and carboxyl groups for enhanced uranium removal from aqueous medium. Microporous and Mesoporous Materials,. **226**: p. 117-124.
19. Zhao, X.S., G. Lu, and G.J. Millar, (1996) Advances in mesoporous molecular sieve MCM-41. Industrial & Engineering Chemistry Research,. **35**(7): p. 2075-2090.
20. Karthikeyan, G. and A. Pandurangan, (2009) Heteropolyacid (H3PW12O40) supported MCM-41: An efficient solid acid catalyst for the green synthesis of xanthenedione derivatives. *Journal of Molecular Catalysis A: Chemical*,. **311**(1-2): p. 36-45.
21. Qin, J., et al., (2015) Synthesis, characterization and catalytic performance of well-ordered mesoporous Ni-MCM-41 with high nickel content. Microporous and Mesoporous Materials,. **208**: p. 181-187.
22. Rojas-Buzo, S., P. García-García, and A. Corma, (2019) Zr-MOF-808@ MCM-41 catalyzed phosgene-free synthesis of polyurethane precursors. Catalysis Science & Technology,. **9**(1): p. 146-156.
23. Brasil, H., et al., (2020)Preparation of novel mesoporous Ca/P MCM-41-based materials for mechanochemical diphenyl sulfide oxidation. Microporous and Mesoporous Materials,. **297**: p. 110017.
24. Wongsakulphasatch, S., et al., (2014) The adsorption aspect of Cu2+ and Zn2+ on MCM-41 and SDS-modified MCM-41. Inorganic Chemistry Communications,. **46**: p. 301-304.
25. Corma, A., et al., (1994) Acidity and stability of MCM-41 crystalline aluminosilicates. *Journal of Catalysis*,. **148**(2): p. 569-574.
26. Gusev, V.Y., et al., (1996) Mechanical stability of pure silica mesoporous MCM-41 by nitrogen adsorption and small-angle X-ray diffraction measurements. *The Journal of Physical Chemistry*,. **100**(6): p. 1985-1988.
27. Galarneau, A., et al., (2008) .Pore-shape effects in determination of pore size of ordered mesoporous silicas by mercury intrusion. *The Journal of Physical Chemistry C*, **112**(33): p. 12921-12927.
28. Izumi, Y., et al., *Silica-included heteropoly compounds as solid acid catalysts.* Microporous Materials, 1995. **5**(4): p. 255-262.
29. Jha, A., et al., (2012) MCM-41 supported phosphotungstic acid for the hydroxyalkylation of phenol to phenolphthalein. Industrial & engineering chemistry research,. **51**(10): p. 3916-3922.
30. Chen, C.-L., et al., (2001) Sulfated zirconia catalyst supported on MCM-41 mesoporous molecular sieve. Applied Catalysis A: General,. **215**(1-2): p. 21-30.

31. Wang, J.-H. and C.-Y. Mou, (2008) Characterizations of aluminum-promoted sulfated zirconia on mesoporous MCM-41 silica: Butane isomerization. Microporous and Mesoporous Materials,. **110**(2-3): p. 260-270.
32. Jiménez-Morales, I., et al., (2011) Calcined zirconium sulfate supported on MCM-41 silica as acid catalyst for ethanolysis of sunflower oil. Applied Catalysis B: Environmental,. **103**(1-2): p. 91-98.
33. Parida, K. and D. Rath, (2006) Studies on MCM-41: Effect of sulfate on nitration of phenol. *Journal of Molecular Catalysis A: Chemical*,. **258**(1-2): p. 381-387.
34. Wang, B., et al., (2004) Sulfamic acid as a green, efficient, recyclable and reusable catalyst for direct addition of aliphatic acid with cyclic olefins. Catalysis letters,. **96**: p. 71-74.
35. Jin, T.-S., et al., (2002) An efficient and convenient procedure for the preparation of 1, 1-diacetates from aldehydes catalyzed by H2NSO3H. Green Chemistry,. **4**(3): p. 255-256.
36. Upadhyaya, D.J., et al., (2007) Efficient, solventless N-Boc protection of amines carried out at room temperature using sulfamic acid as recyclable catalyst. Tetrahedron Letters,. **48**(47): p. 8318-8322.
37. Wang, B., L.-M. Yang, and J.-S. Suo, (2003) Solvent-free tetrahydropyranylation of alcohols with sulfamic acid as reusable catalyst. Synthetic communications,. **33**(22): p. 3929-3934.
38. Kassaee, M.Z., H. Masrouri, and F. Movahedi, (2011) .Sulfamic acid-functionalized magnetic Fe3O4 nanoparticles as an efficient and reusable catalyst for one-pot synthesis of α-amino nitriles in water. Applied Catalysis A: General, **395**(1-2): p. 28-33.
39. Ahmad, M., et al., (2002) Performance and photostability of xanthene and pyrromethene laser dyes in sol-gel phases. *Journal of Physics D: Applied Physics*,. **35**(13): p. 1473.
40. Bhowmik, B.B. and P. Ganguly, (2005) Photophysics of xanthene dyes in surfactant solution. Spectrochimica Acta Part A: Molecular and Biomolecular Spectroscopy,. **61**(9): p. 1997-2003.
41. Knight, C.G. and T. Stephens, (1989) Xanthenedyelabelledphosphatidylethanolamines as probes of interfacial pH. Studies in phospholipid vesicles. *Biochemical Journal*,. **258**(3): p. 683-687.
42. Bruno, O., et al., (2004) Synthesis and pharmacological evaluation of 5H-[1] benzopyrano [4, 3-d] pyrimidines effective as antiplatelet/analgesic agents. Bioorganic & medicinal chemistry,. **12**(3): p. 553-561.
43. Anbia, M., K. Kargosha, and S. Khoshbooei, (2015) Heavy metal ions removal from aqueous media by modified magnetic mesoporous silica MCM-48. Chemical Engineering Research and Design,. **93**: p. 779-788.
44. Hassan, S.M., A.I. Ahmed, and M.A. Mannaa, (2019) Preparation and characterization of SnO2 doped TiO2 nanoparticles: Effect of phase changes on the photocatalytic and catalytic activity. *Journal of Science: Advanced Materials and Devices*,. **4**(3): p. 400-412.
45. Hassan, S., M. Mannaa, and A.A. Ibrahim, (2019) Nano-sized mesoporous phosphated tin oxide as an efficient solid acid catalyst. RSC advances,. **9**(2): p. 810-818.
46. Ibrahim, A.A., S.M. Hassan, and M.A. Mannaa, (2020) Mesoporous tin oxide-supported phosphomolybdic acid as high performance acid catalysts for the synthesis of hydroquinone diacetate. Colloids and Surfaces A: Physicochemical and Engineering Aspects,. **586**: p. 124248.
47. Khder, A., et al., (2008) Surface characterization and catalytic activity of sulfated tin oxide catalyst. Catalysis Communications,. **9**(5): p. 769-777.
48. El-Hakam, S.A., et al., (2018) Synthesis of sulfamic acid supported on Cr-MIL-101 as a heterogeneous acid catalyst and efficient adsorbent for methyl orange dye. RSC advances,. **8**(37): p. 20517-20533.
49. Salama, R.S., S.M. El-Bahy, and M.A. Mannaa, (2021) Sulfamic acid supported on mesoporous MCM-41 as a novel, efficient and reusable heterogenous solid

acid catalyst for synthesis of xanthene, dihydropyrimidinone and coumarin derivatives. Colloids and Surfaces A: Physicochemical and Engineering Aspects,. **628**: p. 127261.
50. Salam, M.S.A., et al., (2015) Synthesis and characterization of MCM-41-supported nano zirconia catalysts. Egyptian *Journal of Petroleum,*. **24**(1): p. 49-57.
51. Kannan, B., et al., (2013) Growth and characterisation of lanthanum doped sulphamic acid single crystal. *Indian J Sci Technol,*. **6**: p. 4357-61.
52. Li, X., et al., (2014) Cr (VI) Removal from Aqueous by Adsorption on Amine-Functionalized Mesoporous Silica Prepared from Silica Fume. J*ournal of Chemistry,*. **2014**(1): p. 765856.
53. Ibrahim, A.A., et al., (2021) Synthesis of sulfated zirconium supported MCM-41 composite with high-rate adsorption of methylene blue and excellent heterogeneous catalyst. Colloids and Surfaces A: Physicochemical and Engineering Aspects,. **616**: p. 126361.
54. Hassan, S.M., A.I. Ahmed, and M.A. Mannaa, (2019) Surface acidity, catalytic and photocatalytic activities of new type H3PW12O40/Sn-TiO2 nanoparticles. Colloids and Surfaces A: Physicochemical and Engineering Aspects,. **577**: p. 147-157.
55. Hassan, S., et al., (2013) Surface acidity and catalytic activity of phosphomolybdic acid/SnO2 catalysts. *Int. J. Modern Chem,*. **4**(2): p. 104-116.
56. Ho, K.Y., G. McKay, and K.L. Yeung, (2003) Selective adsorbents from ordered mesoporous silica. Langmuir,. **19**(7): p. 3019-3024.
57. Al-Ghouti, M.A., et al., (2010) Adsorption mechanisms of removing heavy metals and dyes from aqueous solution using date pits solid adsorbent. *Journal of hazardous materials,*. **176**(1-3): p. 510-520.